

Integration of hydrogeophysical datasets and empirical orthogonal functions for improved irrigation water management

Catherine E. Finkenbiner^{1,3} · Trenton E. Franz¹ · Justin Gibson¹ · Derek M. Heeren² · Joe Luck²

© Springer Science+Business Media, LLC, part of Springer Nature 2018

Abstract Precision agriculture offers the technologies to manage for infield variability and incorporate variability into irrigation management decisions. The major limitation of this technology often lies in the reconciliation of disparate data sources and the generation of irrigation prescription maps. Here the authors explore the utility of the cosmic-ray neutron probe (CRNP) which measures volumetric soil water content (SWC) in the top ~ 30 cm of the soil profile. The key advantages of CRNP is that the sensor is passive, non-invasive, mobile and soil temperature-invariant, making data collection more compatible with existing farm operations and extending the mapping period. The objectives of this study were to: (1) improve the delineation of irrigation management zones within a field and (2) estimate spatial soil hydraulic properties to make effective irrigation prescriptions. Ten CRNP SWC surveys were collected in a 53-ha field in Nebraska. The SWC surveys were analyzed using Empirical Orthogonal Functions (EOFs) to isolate the underlying spatial structure. A statistical bootstrapping analysis confirmed the CRNP+EOF provided superior soil hydraulic property estimates, compared to other hydrogeophysical datasets, when linearly correlated to laboratory measured soil hydraulic properties (field capacity estimates reduced 20–25% in root mean square error). The authors propose a soil sampling strategy for better quantifying soil hydraulic properties using CRNP+EOF methods. Here, five CRNP surveys and 6–8 sample locations for laboratory analysis were sufficient to describe the spatial distribution of soil hydraulic properties within this field. While the proposed strategy may increase overall effort, rising scrutiny for agricultural water-use could make this technology cost-effective.

✉ Catherine E. Finkenbiner
c.finkenbiner@gmail.com

Trenton E. Franz
tfranz2@unl.edu

¹ School of Natural Resources, University of Nebraska-Lincoln, Lincoln, USA

² Department of Biological Systems Engineering, University of Nebraska-Lincoln, Lincoln, USA

³ Present Address: Department of Biological & Ecological Engineering, Oregon State University, Corvallis, USA

Keywords Water use efficiency · Soil hydraulic parameters · Irrigation management · Soil spatial variability

Introduction

Water scarcity is predicted to be the major limitation to increasing agronomic outputs to meet future food and fiber demands (UNDP 2007). With the agricultural sector accounting for 80–90% of all consumptive water use and an average water use efficiency of less than 45% (Hezarjaribi and Sourell 2007; Molden 2007), major advances must be made in irrigation water management. Currently, irrigation is a key component of global food security, accounting for ~40% of global food production and ~20% of all arable land (Molden 2007; Schultz et al. 2005). Precision agriculture offers the technologies to address and manage for infield variability and incorporate that variability into management decisions (Howell et al. 2012).

According to a 2012 U.S. Department of Agriculture (USDA) Census of Agriculture report, Nebraska ranks first nationally in irrigated area approximately 3.4 million irrigated hectares, and about 70% of that area has center pivot irrigation (USDA 2012). Conventional center pivot systems manage a field as a uniform unit, thus ignoring the heterogeneity across the field, and often management decisions are based on average field conditions (i.e. average soil hydraulic properties, average soil water content (SWC); McCarthy et al. 2014). Consequently, expected crop yield may differ in sub-regions of a field due to variations in SWC and physical properties. Variable-rate irrigation (VRI) and variable-speed irrigation (VSI) systems can vary application depth in relation to the spatial variability of soil properties (Hezarjaribi and Sourell 2007). VSI varies the speed of the pivot to adjust application depth in sectors and VRI uses nozzle control to vary application depth in irregularly shaped management zones. Additionally, fertigation inputs can be managed for site-specific field conditions and soil properties to ensure minimal chemical loss in the runoff (Hedley 2015). Due to the high temporal variability in SWC, the incorporation of VRI has the potential to increase crop water use efficiency and yield (Haghverdi et al. 2015b). The major limitation to implementing this technology often lies in the management of spatial datasets and the writing of irrigation prescription maps that address variables impacting yield and SWC (Evans et al. 1996; Howell et al. 2012). This requires efficient and accurate methods for measuring the subfield scale spatial variability of soil properties including porosity, saturated hydraulic conductivity, unsaturated hydraulic conductivity, available water, texture and depth (Hezarjaribi and Sourell 2007; Pan et al. 2013; Ranney et al. 2015). Managing irrigation rates and times based on hydraulic properties allows for irrigators to prescribe application depths based on the SWC below field capacity and above maximum allowable depletion.

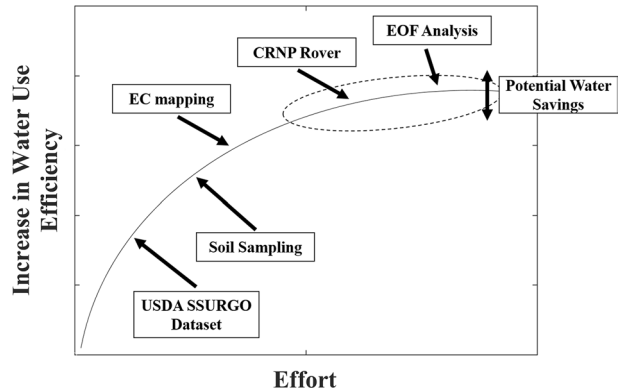
Land managers use several methods to address and manage for in-field variability and to delineate irrigation management zones (IMZs) including available soil spatial datasets, yield maps, electrical resistivity/conductivity (EC) surveys, and commercially available instruments. Unfortunately, soil spatial datasets are often not at resolutions appropriate for field-scale management (Bobryk et al. 2016). One strategy land managers use is the delineation of IMZs within a field based on EC surveys. High resolution spatiotemporal modeling using EC surveys has been used to characterize dynamic SWC patterns in relation to crop needs (Hedley et al. 2013). Unfortunately, EC is sensitive to temperature, SWC, texture, clay content and salinity (Haghverdi et al. 2015a; Rodriguez-Perez et al. 2011), thus

making exact boundary determination challenging. Most EC systems are used to delineate management zones only after harvest and before planting in nonfrozen soils, thus limiting mapping opportunities in cold climates. While changes in SWC do account for over 50% of variability in soil EC readings (Brevik et al. 2006), the dynamic nature of SWC causes EC and clay measurements to vary temporally (McCutcheon et al. 2006) making the use of a single EC survey problematic. Martini et al. (2016) investigated this temporal variability and emphasized the importance of multiple surveys to capture the dynamic SWC patterns represented by EC surveys. Other impacting factors, beyond SWC, include groundwater levels and the concentration of the pore water solution, which influence the electrical conductance pathway (Martini et al. 2016). Additional commercially available methodologies are available for measuring soil physical variability, however they were not explored in this study [e.g. Trimble Soil Information System (SIS) (Trimble Inc., Sunnyvale, CA)].

Beyond EC surveys, other hydrogeophysical instruments (see e.g. Binley et al. 2015; Coopersmith et al. 2014; Franz et al. 2016; Villarreyes et al. 2011) offer promising opportunities in precision agriculture. One such instrument to be explored in this work is the cosmic-ray neutron probe (CRNP), which has been used within agricultural systems to approximate SWC at the field- to small-watershed-scale (Franz et al. 2015). The CRNP detects epithermal neutron energies reflected from the soil, which are inversely related to SWC (Zreda et al. 2012). For this study, the CRNP was used to measure SWC at high spatial and temporal resolutions to characterize its dynamic nature over the growing season. One key advantage to using the passive, non-invasive, and soil-temperature-invariant CRNP method is that SWC data can be collected using a wide variety of commercially available vehicles from harvest until the following season when the crop is too tall for the vehicle (~0.20 m for this work). While not performed here, CRNP surveys, mobile CRNP measurements, with taller crop heights can easily be collected from taller-bodied farm equipment (e.g. tractor, sprayer, etc.). For this work, a standard multivariate analysis, Empirical Orthogonal Functions [EOF, (Perry and Niemann 2006)], was used to characterize the spatial variability of SWC across the study site using CRNP surveys collected between 2015 and 2016. EOF analyses have been proven to be an accurate method for large sample sizes or more than 5 days of SWC monitoring (Werbylo and Niemann 2014). Within intensely monitored agricultural systems, EOF analysis has also been used to identify dominant parameters controlling spatial and temporal patterns of surface SWC without being affected by a single random process (Korres et al. 2010). Furthermore, EOF analysis provides a framework to estimate underlying SWC variations constructed using historical SWC observations to forecast SWC patterns for unobserved times.

The objectives of this study were to: (1) improve the delineation of management zones within a field and (2) estimate the relevant spatially-distributed soil hydraulic properties (i.e. field capacity and wilting point) to inform irrigation prescriptions. Laboratory measured hydraulic parameters were compared to values from the USDA soil survey dataset, then correlated with an EC map, and then to the CRNP-derived EOF surface. Lastly, a cross validation bootstrapping analysis was performed to compare and contrast the various candidate environmental covariates. The CRNP surveys, when combined with the EOF analysis, were hypothesized to be the best predictor of soil hydraulic property spatial variability compared to traditional and widely-used methods. It was also hypothesized that the EOF surface would be a good candidate for more accurately delineating IMZs. To illustrate the potential increase in water use efficiency versus effort (i.e. time, energy, and cost) of the various strategies discussed, Fig. 1 presents a conceptual diagram with a set of existing technologies/methodologies. The figure serves as a guide to the reader and will be further discussed later in this paper with respect to the specific findings from this field site.

Fig. 1 Conceptual diagram of potential increase in water use efficiency versus effort for various soil hydraulic datasets/techniques



Materials and methods

Study site

The selected study site is a 53-ha field (circle with ~400 m radius) irrigated with a variable-rate irrigation (VRI) pivot near Sutherland, NE (41.065393°, -101.102663°) (Fig. 2). The field contains significant topo-edaphic gradients, i.e. soil and topographic properties, making it an ideal candidate for VRI. Figure 2 illustrates the elevation (provided by a local crop consultant using a Real Time Kinematic (RTK) Global Positioning System (GPS)) and topographic wetness index (TWI) of the study site. The TWI calculates SWC spatial patterns based on the up-slope contribution area and slope (Sorensen et al. 2006). The field was planted with soybean (*Glycine max* L.) in 2014 and popcorn maize (*Zea Mays var. everta*) from 2015 to 2016. The soybean yield averaged ~3.8 Mg/ha and the popcorn yields averaged ~5.3 Mg/ha. Using data from an Automated Weather Data Network (AWDN) site located near North Platte, NE (~40 km from study site), the authors estimated annual temperature highs to be around 18 °C and lows to be about 2 °C (<http://www.hprcc.unl.edu/awdn.php>, Accessed 25 January 2017). The authors used the AWDN dataset to estimate decadal annual average precipitation at 445 mm year⁻¹ with 325 mm falling between May and September. Additionally, the authors estimated potential annual evapotranspiration to be at 1475 mm year⁻¹ with 925 mm occurring between May and September. According to the local producer, applied irrigation varies between 150 and 300 mm year⁻¹ depending on the year. Soil classifications from the available USDA SSURGO (Soil Survey Staff 2016) spatial and tabular dataset were used to estimate texture and soil hydraulic properties at the study site. SWC at field capacity (cm³ cm⁻³), correlating to a soil water pressure of -33 kPa, and wilting point (cm³ cm⁻³), correlating to a soil water pressure of -1500 kPa, were averaged for each of the map units from 0 to 0.3 m (Fig. 3). The USDA SSURGO database delineated contiguous areas with similar soils as a single map unit. In general, the eastern region of the field has sandier soils and the western region is a mixture of sandy and silt loams. The field has a wide gradient in field capacity (0.090–0.307 cm³ cm⁻³) and wilting point (0.027–0.164 cm³ cm⁻³) values depending on soil classification. The TWI product (Fig. 2) correlates well with the classifications from the SSURGO dataset with wetter regions of the field relating to finer soil textures.

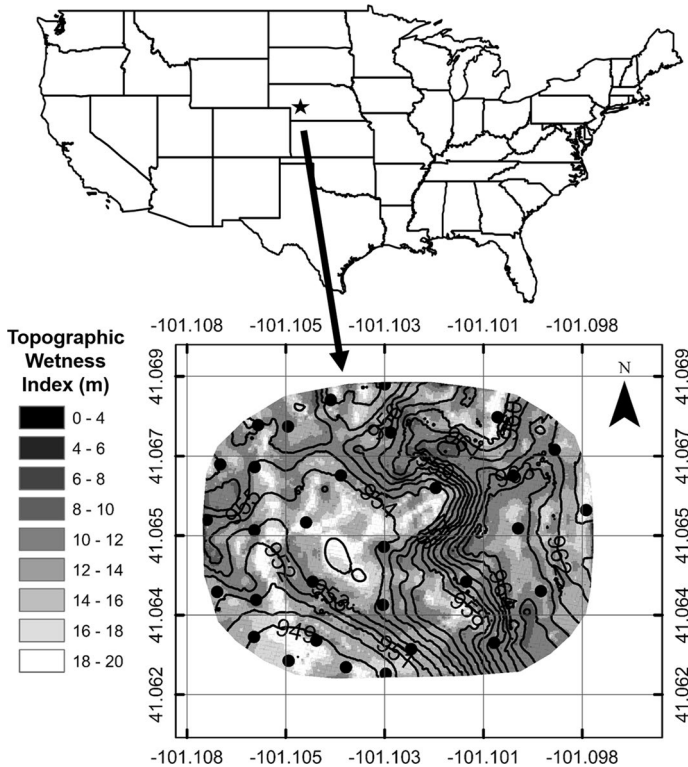


Fig. 2 Field site located near Sutherland, NE (field center: 41.065393° , -101.102663°), illustrating latitude, longitude, soil core sampling locations (black dots), 1 m elevation contours, and the calculated topographic wetness index (TWI) (m)

Hydrogeophysical datasets

An electrical conductivity (EC) survey measuring bulk apparent electrical conductivity (EC_a , $mS\ m^{-1}$) was collected on 24 February 2016 using a DUALEM-21S sensor (DUALEM, Milton, Canada). The DUALEM sensor has dual-geometry receivers at separations of 1 and 2.1 m from the transmitter, which provided four simultaneous depth estimates of EC_a every second (DuaLEM Inc. 2013). The ~ 2.1 m horizontal co-planar sensor estimated EC_a values for this study (see DUALEM manual for approximate depth of exploration curves for each sensor configuration). The DUALEM was towed behind an all-terrain vehicle (ATV) on a plastic sled at speeds of $8\text{--}15\ km\ h^{-1}$ with $\sim 7\text{--}9$ m spacing, taking about 75 min to complete the survey. A Hemisphere GPS XF101 DGPS (Juniper Systems, Inc., Logan, UT) unit recorded the location of each measurement. Following basic quality assurance and quality control of the raw EC_a data (Franz et al. 2011), a spatial map with 5 by 5 m resolution was created using an inverse-distance weighting procedure.

Ten mobile cosmic-ray neutron probe (CRNP) surveys to estimate soil water content (SWC) were completed at the site from March 2015–June 2016 using an ATV driven in a similar pattern and rate as the previously described EC survey. The mobile CRNP records epithermal neutron intensity integrated over one-minute counting intervals. The change in epithermal neutron intensity is inversely correlated to the mass of hydrogen

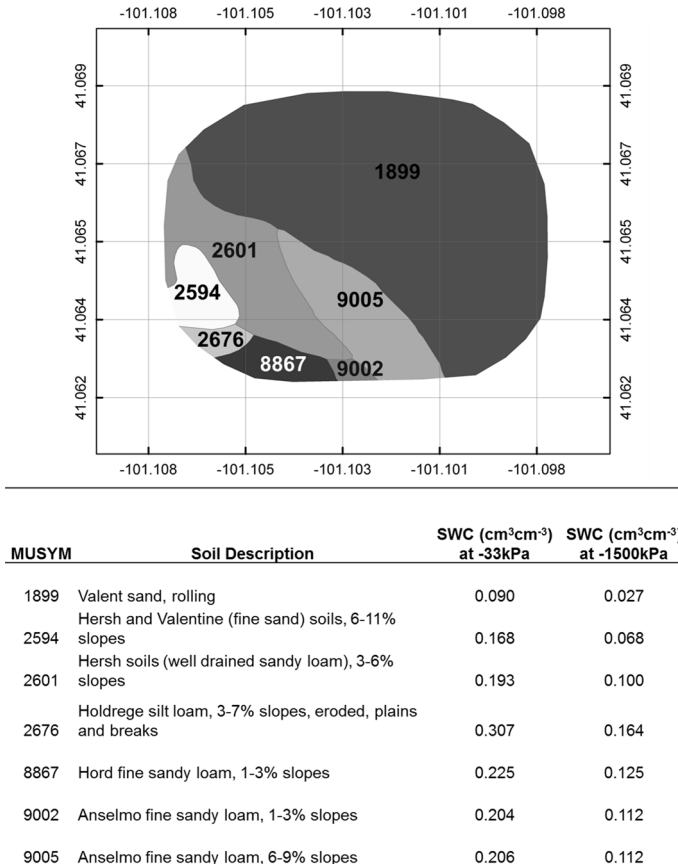


Fig. 3 The USDA SSURGO map unit key (MUKEY), soil descriptions, and their respective SWC at field capacity and wilting point. According to the World Reference Base (WRB) FAO soil classifications, the soils are a luvis kastanozem

in the measurement volume (Zreda et al. 2012). A main advantage of the CRNP survey, when compared to the EC survey, is the temperature-invariance. The CRNP method has no interaction with the electromagnetic atom shells and the neutrons interact with the atomic nuclei instead. The soil's atomic energy variation due to ambient temperature changes is negligible compared to the epithermal neutron intensities (see Glasstone and Edlund 1952 for a description of neutron scattering cross section temperature dependence and Campbell et al. 1948 for a description of electrical conductivity temperature dependence). Depending on local conditions (i.e. elevation, water vapor, AWC, etc.), the CRNP measurement volume is roughly a disk, with a 130–250 m radius circle and penetration depth of 0.15–0.40 m (Köhli et al. 2015). For simplicity, a constant penetration depth of 0.3 m was assumed for all surveys. Atmospheric hydrogen pools within the CRNP footprint were accounted for by a relative humidity and temperature sensor mounted on the ATV. Lattice water, soil organic carbon equivalent and bulk density were measured at 0.015, 0.0083, and 1.62 g cm⁻³, respectively. Interference of the biomass in the total CRNP measurement volume was considered negligible because the surveys were collected over bare soil or when the crop height was less than 0.20 m. The authors note that SWC changes are by far the

largest change in hydrogen mass within the measurement footprint (McJannet et al. 2014). Numerous validation studies across the globe (see e.g. Bogen et al. 2013; Hawdon et al. 2014; Franz et al. 2015, 2016; Iwema et al. 2017, among others) have shown the CRNP to have area-average measurement accuracies of less than $0.03 \text{ cm}^3 \text{ cm}^{-3}$ against a variety of industry standard SWC point scale probes. The calculated SWC within the measurement volume in a non-linearly weighed average with increased sensitivity near the CRNP (Schrön et al. 2017). In order to provide a SWC map, first a spatial map of neutron intensity was estimated, then a calibration function was applied following details in Franz et al. (2015) for agricultural fields. The neutron intensity map is created in two steps. First, a drop-in-the-bucket preprocessing step is applied, where a dense grid is generated (here 20 by 20 m) and all raw data points are found within a certain radius (here 50 m). The size of the processing grid and average radius were varied in order to minimize any spatial interpolation artifacts (i.e. bulls eyes around observations points). Note, that future work should investigate how the size of the CRNP measurement disk, non-linear weighting of neutron intensity, and underlying length scale of soil heterogeneity affect the spatial interpolation algorithm. However, this was beyond the scope of the current study. Following the selection of grid size and search radius, the average of all raw data found within the search radius is assigned to the grid center. This oversampling approach is necessary for sharpening the image quality and is a common strategy used in remote sensing analyses (see Chan and Njoku 2014) when overlapping area average observations are collected, like the CRNP in this study. Next, an inverse-distance-weighted approach is used on the resampled 20 m grid to provide the 5-m neutron intensity estimate. Finally, the neutron intensity gridded estimate is converted to SWC following Franz et al. (2015). The authors refer the reader to the rapidly growing CRNP literature (see Zreda et al. 2012) instead of providing full details of the methodology here.

Soil sampling and laboratory analysis

Thirty-one sample locations (Fig. 2) were chosen based on the SSURGO database soil classifications, EC map and EOF analysis in a stratified random sampling scheme. Undisturbed soil cores (250 cm^3) were collected inside stainless steel cylinders at $\sim 0.2 \text{ m}$ depth at each sample location. The soil cores were placed in a cooler and transported back to the laboratory where they were stored in a $4 \text{ }^\circ\text{C}$ refrigerator for later analysis. Soil water retention curves were estimated for each of the soil cores using a Decagon HYPROP (Decagon Devices, Pullman, WA, USA). Saturated soil samples were exposed to evaporation in the laboratory and weighed throughout the experiment. Evaporation methods are proven to be a fast and reliable method for determining soil hydraulic properties within the saturated to moderate SWC range (Peters and Durner 2008; Schindler et al. 2010). The matric potential was continuously monitored by two tensiometers inserted at the base of the soil cores at two different lengths within the core. The tensiometers and instrument bases were degassed using a vacuum pump. The HYPROP software (Decagon Devices, Pullman, WA, USA) calculated data points along the retention curve and unsaturated hydraulic conductivity curve. An average measured bulk density of 1.62 g cm^{-3} and porosity of 38.9% were assigned for each of the undisturbed samples to generate soil water retention curves. Following the HYPROP analysis, a WP4C Dewpoint Potential Meter (Decagon Devices, Pullman, WA, USA) was used to approximate tension for the moderate to dry SWC ranges. The soil cores were dried at $105 \text{ }^\circ\text{C}$ for 24 h before collecting 1–9 sub-samples per sample. Varying volumes of water were added to the sub-samples to obtain SWC near wilting point and to further characterize the soil water retention curves. The sub-samples were sealed for

24 h after water was added to allow for the water to disperse evenly throughout the subsample. Inside the measurement chamber of the WP4C, the dew point temperature of the moist air was measured by a chilled mirror and the sample temperature was measured by an infrared thermometer. Those two values were then used to calculate relative humidity and thus, potential of the soil water. The WP4C has an accuracy of ± 0.05 MPa from 0 to -5 MPa and 1% from -5 to -300 MPa (Decagon Devices, Inc. 2015).

Statistical analysis

In order to illuminate the underlying spatial variability of the SWC maps, an empirical orthogonal function (EOF) analysis was used on the ten CRNP SWC maps. Full details on the multivariate statistical EOF analysis are provided elsewhere (Korres et al. 2010; Perry and Niemann 2006) and only a brief summary is provided here. The EOF analysis decomposes the observed SWC variability measured by the CRNP surveys into a set of orthogonal spatial patterns (EOFs), which are invariant in time, and a set of time series called expansion coefficients, which are invariant in space (Perry and Niemann 2006). Multiplication of the EOFs and expansion coefficients will exactly reconstruct the original pattern. Often the number of needed coefficients (i.e. eigenvectors) to reconstruct most of the data is less than the original dataset (i.e. determined by the ranked eigenvalues), thus the procedure can be used as a way to reduce the dimensionality of the dataset while preserving the key information. The authors note that EOF is nearly identical to Principal Component Analysis save the splitting of axis of variation into spatial and temporal coefficients instead of arbitrary linear combinations.

A bootstrap validation analysis was used to: (1) determine the accuracy of the regressed hydraulic parameter to the measured hydraulic parameter and (2) determine how many soil samples and their corresponding hydraulic parameters were required for the root mean square error (RMSE) to converge. The hydrogeophysical datasets explored for this analysis were the CRNP EOF surface derived from the SWC surveys, the CRNP EOF surface derived from the corrected neutron counts (i.e. pressure, intensity, and water vapor corrections), ECa survey and elevation. Each hydrogeophysical dataset was randomly divided into a training set, ranging in size from 3 to 30, and a testing set for 1000 random iterations. The training sets and their corresponding laboratory measured soil hydraulic properties (i.e. field capacity, wilting point, available water content (AWC)) were used to build a simple linear model to predict the remaining laboratory measured soil hydraulic property values. The mean RMSE and standard deviation of the RMSE for the 1000 simulations were calculated for the predicted hydraulic property values and the laboratory measured soil hydraulic property values. This analysis followed similar methods from Gibson and Franz (2018).

Results and discussion

Hydrogeophysical mapping and EOF analysis

The apparent electrical conductivity (ECa) map for the field is illustrated in Fig. 4 and provides additional spatial information on soil texture variability as compared to the USDA SSURGO map (Fig. 3). This type of information has been used for the delineation of irrigation management zones (IMZs; Pan et al. 2013). As noted previously, the ECa

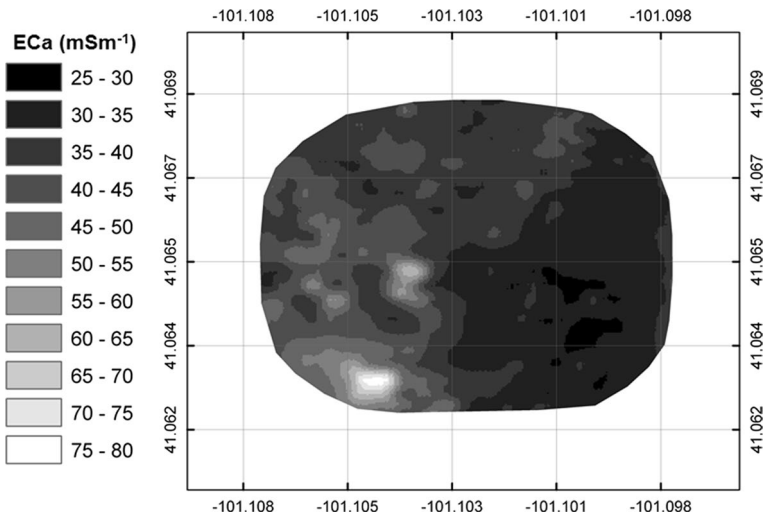


Fig. 4 Apparent bulk electrical conductivity map (ECa) collected on 24 February 2016 using a Dualem-21S sensor

map is subject to field conditions at the time of the sampling (Martini et al. 2016). Therefore, areas of high EC measurements in the southwest quadrant of the field may be due to increased soil cations, soil water content (SWC), and/or temperature anomalies at the time of sampling. At a first glance, the delineated soil boundary by the USDA SSURGO database displays some spatial correlation to the ECa map. However, there is high variability of ECa values within each USDA SSURGO soil classification, which has been observed in other research (Brevik et al. 2006). Thus, the soil classification from the SSURGO dataset may or may not be the appropriate boundaries for irrigation management zones (IMZs) within the field. This uncertainty of exact IMZ boundaries and questionable repeatability of ECa makes this method problematic, particularly given the high initial capital for precision agricultural equipment. The result here suggests the use of soil survey datasets and ECa be used in tandem to delineate IMZs for precision agriculture, which is supported by the results of Brevik et al. (2006).

Figure 5 illustrates the large spatiotemporal variation in SWC over the ten dates observed using the CRNP rover. Despite regions of the field with finer soil textures and higher ECa generally having a higher SWC in each of the soil moisture maps, there is inconsistency in the spatial distribution of the SWC. For example, compare the SWC spatial distribution for the survey dates of June 10, 2015 and May 11, 2016. Table 1 summarizes the SWC minimum, maximum, mean and standard deviation for each CRNP survey date in Fig. 5. The ten CRNP rover surveys were used to perform Empirical Orthogonal Function (EOF) analysis. Figure 6 illustrates the first and second EOF coefficients at the study site. The EOF analysis contextualizes the behavior of the SWC (and thus underlying soil hydraulic properties) at any given point in the field relative to the mean SWC as a whole. Therefore, points in the field that are relatively wet persistently will have positive coefficients and points in the field that are relatively dry will have negative coefficients. Here the first EOF coefficients explained 79.6% of the spatial SWC variability followed by 5.6% explained by the second EOF. Therefore, only the first EOF was considered in the subsequent analyses. Statistical bootstrapping of the SWC indicated that five CRNP surveys at different SWC

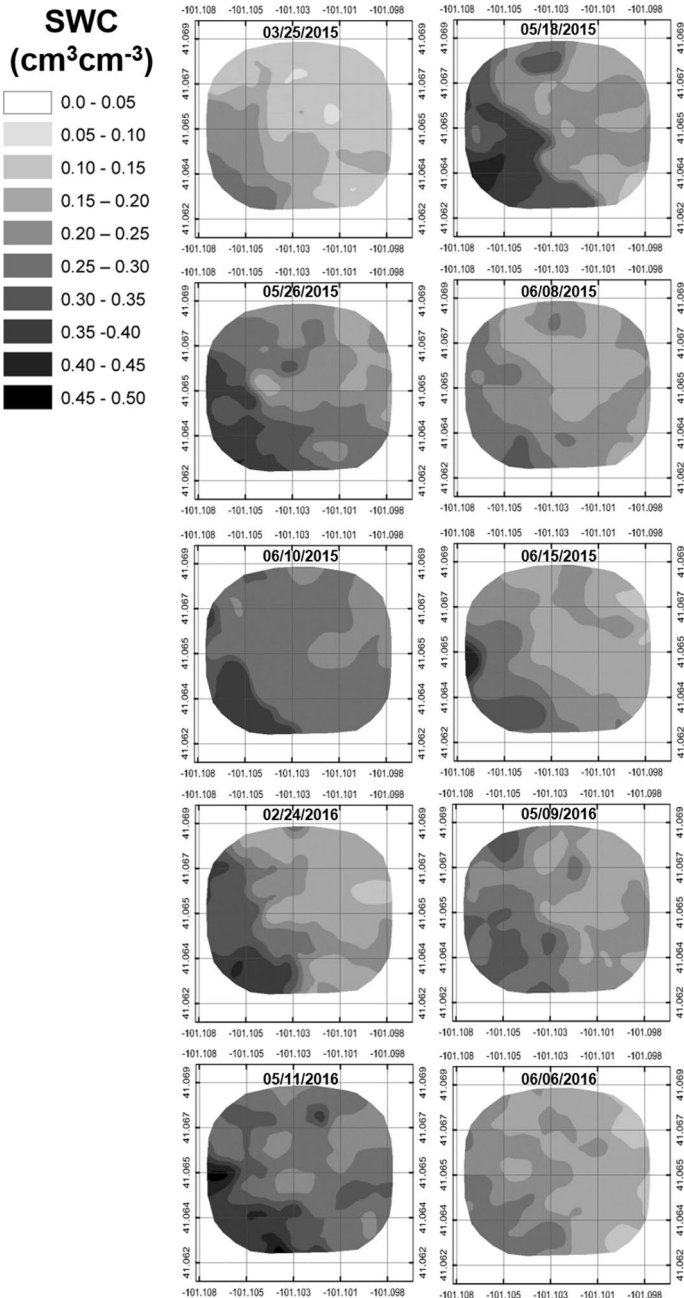


Fig. 5 Ten CRNP rover SWC surveys collected between March 2015 and June 2016 (see Table 1)

conditions were sufficient to estimate the first EOF coefficients to within 5% of the values using data from all ten surveys. This reduction in required number of CRNP surveys is critical for economic considerations beyond a research study (see [“Recommendations for](#)

Table 1 Summary of the minimum SWC, maximum SWC, mean SWC and SWC standard deviation (SD) for the ten CRNP surveys (Fig. 5)

CRNP survey date	Minimum (cm ³ cm ⁻³)	Maximum (cm ³ cm ⁻³)	Mean (cm ³ cm ⁻³)	SD (cm ³ cm ⁻³)
03/25/15	0.082	0.318	0.162	0.055
05/18/15	0.116	0.388	0.244	0.062
05/26/15	0.162	0.449	0.274	0.065
06/08/15	0.127	0.336	0.220	0.041
06/10/15	0.101	0.412	0.247	0.059
06/15/15	0.102	0.455	0.225	0.062
02/24/16	0.124	0.376	0.223	0.060
05/09/16	0.157	0.369	0.241	0.052
05/11/16	0.185	0.491	0.300	0.059
06/06/16	0.124	0.302	0.201	0.045

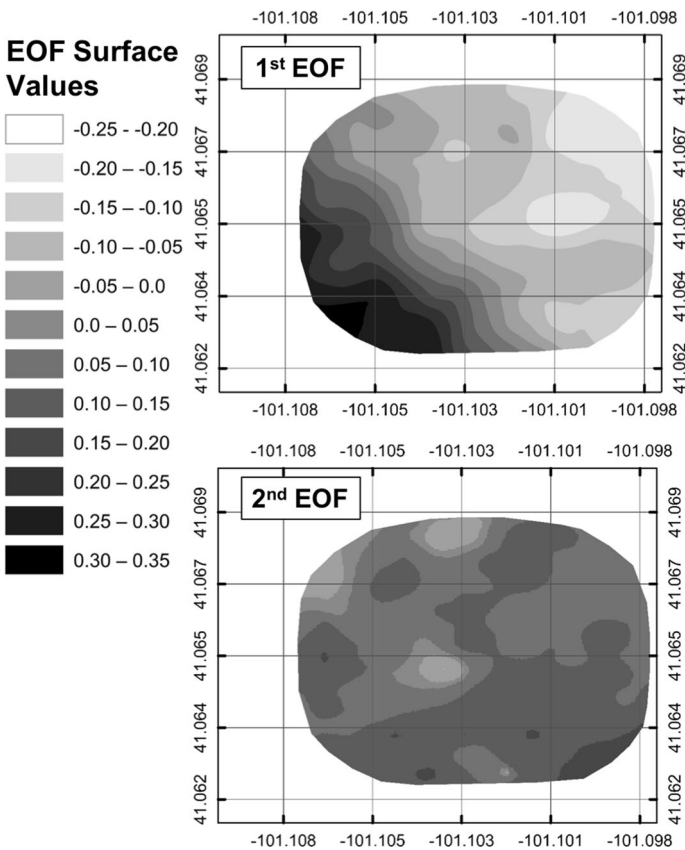


Fig. 6 The first EOF surface depicting the underlying dominant spatial structure created from the ten CRNP rover SWC surveys in Fig. 5 and Table 1

future soil hydraulic property sampling”). The first EOF map provides detailed information for the delineation of IMZs. Given the removal of the time-varying component of the signal the authors argue that the map is a superior method to delineate IMZs as compared to the USDA SSURGO dataset and ECa mapping. The first EOF map is a continuous surface; thus, it can be applied at a variety of spatial scales and used within existing agricultural management software (such as a shapefile input). The remaining questions are: (1) is the EOF map a better predictor of soil hydraulic property spatial variation compared to the SSURGO database and ECa maps and (2) is the information provided by an EOF map economical for a producer to implement into current agricultural practices?

Soil hydraulic properties from sampling analysis

Using each of the thirty-one undisturbed soil cores, soil hydraulic properties were estimated from soil water retention curves generated using the Hyprop software. To illustrate the type of data generated, three of the soil cores from different soil textures and their respective field capacity and wilting point values are shown in Fig. 7. Table 2 summarizes the SWC at field capacity (-33 kPa), SWC at wilting point (-1500 kPa) and calculated available water content (AWC, $\text{cm}^3 \text{cm}^{-3}$) for each of the thirty-one soil cores. AWC was calculated by subtracting the SWC at -1500 kPa from the SWC at -33 kPa. In general, areas of the field with lower EOF values also have lower SWC at field capacity and wilting point. The EOF values are representative of the orthogonality of the SWC spatial patterns, therefore assumptions regarding in-field heterogeneity can be based off of the new EOF surfaces. Additionally, SWC at field capacity and wilting point is higher for finer soils and lower in coarser texture classes. AWC is higher for areas of the field with finer textured soils.

Comparison of landscape position and hydrogeophysical datasets with laboratory analysis

Figure 8 illustrates scatterplots of AWC, elevation, topographic wetness index (TWI), ECa and EOF datasets with the laboratory measured field capacity and wilting point values from

Fig. 7 Soil water retention functions from three undisturbed soil cores. Values before pF (absolute value of the \log_{10} of soil tension, (MPa)) of three were recorded using the Decagon Hyprop and values after a pF of three were recorded using a WP4C Dew-point PotentiaMeter

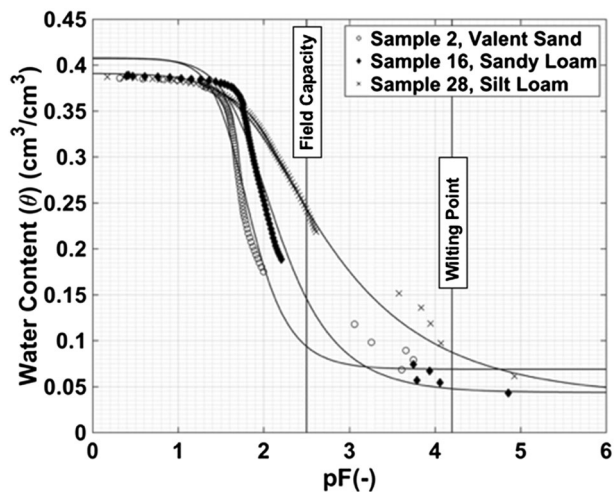


Table 2 Summary of undisturbed soil core locations (latitude, longitude (SW corner: 41.06195°, - 101.10744°), UTM (given relative to SW corner: 322921.5, 4547773.5 14T) and associated values: elevation, topographic wetness index (TWI), SSURGO Map Unit Key (MUKEY), soil water content (SWC) at - 6 kPa, - 33 kPa and - 1500 kPa, and available water content (AWC)

Latitude (°)	Longitude (°)	UTM Zone 14T		SSURGO Database			ECa (mSs ⁻¹)	CRNP EOF (-)	Measured SWC (cm ³ cm ⁻³) at					
		Easting		TWI (m)	MUKEY	SWC (cm ³ cm ⁻³) at 33 kPa			SWC (cm ³ cm ⁻³) at 1500 kPa	6 kPa	33 kPa	1500 kPa	AWC (cm ³ cm ⁻³)	
		Northing	Elevation (m)											
41.06821	- 101.10042	606.7	681.3	958.74	12.73	1899	0.090	0.027	41.20	- 0.1787	0.286	0.096	0.080	0.016
41.06744	- 101.09908	717.3	592.6	961.77	10.49	1899	0.090	0.027	33.36	- 0.1992	0.259	0.092	0.069	0.023
41.06683	- 101.10006	633.7	527.1	962.92	10.09	1899	0.090	0.027	31.73	- 0.1382	0.305	0.112	0.063	0.049
41.06559	- 101.09994	639.9	388.9	964.36	11.78	1899	0.090	0.027	31.12	- 0.1814	0.338	0.225	0.068	0.157
41.06603	- 101.09835	775.0	434.5	960.95	13.59	1899	0.090	0.027	36.07	- 0.1623	0.342	0.152	0.069	0.083
41.06516	- 101.10308	375.3	348.3	954.22	9.00	1899	0.090	0.027	33.49	- 0.0894	0.296	0.104	0.055	0.049
41.06656	- 101.10186	481.0	500.4	954.87	12.84	1899	0.090	0.027	37.28	- 0.0858	0.302	0.111	0.049	0.062
41.06683	- 101.10410	293.8	535.3	954.17	10.30	1899	0.090	0.027	36.22	- 0.0727	0.245	0.080	0.073	0.007
41.06785	- 101.10291	396.5	645.7	957.59	9.70	1899	0.090	0.027	38.11	- 0.0599	0.304	0.050	0.043	0.007
41.06896	- 101.10305	387.4	769.7	954.23	9.23	1899	0.090	0.027	36.75	- 0.0823	0.285	0.078	0.051	0.027
41.06860	- 101.10432	280.5	732.6	953.95	10.17	1899	0.090	0.027	39.07	- 0.0579	0.211	0.083	0.065	0.018
41.06798	- 101.10533	193.9	665.9	956.52	9.27	1899	0.090	0.027	37.89	0.0113	0.270	0.096	0.057	0.039
41.06412	- 101.09939	682.4	224.7	964.24	10.82	1899	0.090	0.027	29.98	- 0.0667	0.302	0.071	0.062	0.009
41.06434	- 101.10115	535.1	253.4	960.25	10.61	1899	0.090	0.027	33.20	- 0.0605	0.315	0.090	0.063	0.027
41.06290	- 101.10051	585.1	92.2	961.18	8.56	1899	0.090	0.027	31.68	- 0.1141	0.264	0.076	0.042	0.034
41.06803	- 101.10603	135.1	672.7	955.85	12.16	1899	0.090	0.027	36.13	0.0007	0.326	0.142	0.048	0.094
41.06704	- 101.10610	126.4	563.2	954.74	11.33	1899	0.090	0.027	43.32	0.0208	0.262	0.109	0.058	0.051
41.06712	- 101.10692	57.7	572.8	955.13	10.41	2601	0.193	0.100	43.84	0.2084	0.347	0.217	0.062	0.155
41.06557	- 101.10611	121.5	399.4	952.97	9.06	2601	0.193	0.100	47.80	0.1812	0.311	0.206	0.090	0.116
41.06436	- 101.10476	232.2	261.9	953.11	8.69	2601	0.193	0.100	36.45	0.1285	0.348	0.175	0.056	0.119
41.06582	- 101.10487	226.5	424.7	953.08	15.14	2601	0.193	0.100	43.80	0.0456	0.322	0.203	0.052	0.151

Table 2 (continued)

Latitude (°)	Longitude (°)	UTM Zone 14T		SSURGO Database		ECa (mSs ⁻¹)	CRNP EOF (-)	Measured SWC (cm ³ cm ⁻³) at				
		Eastings	Northing	Elevation (m)	TWI (m)			MUKEY	SWC (cm ³ cm ⁻³) at 33 kPa	SWC (cm ³ cm ⁻³) at 1500 kPa	6 kPa	33 kPa
41.06378	-101.10311	368.6	195.2	954.26	10.35	9005	0.206	0.1112	0.337	0.222	0.084	0.138
41.06219	-101.10302	372.3	18.0	949.28	12.75	9002	0.206	0.1112	0.341	0.149	0.053	0.096
41.06276	-101.10247	420.2	80.0	952.23	11.45	9005	0.206	0.1112	0.321	0.113	0.044	0.069
41.06235	-101.10396	293.8	37.1	948.56	11.33	8867	0.225	0.125	0.350	0.230	0.070	0.160
41.06296	-101.10466	236.4	107.2	948.52	11.81	8867	0.225	0.125	0.345	0.223	0.054	0.169
41.06249	-101.10531	180.2	55.8	948.14	13.02	8867	0.225	0.125	0.370	0.315	0.078	0.237
41.06306	-101.10612	113.7	120.8	949.00	12.00	2676	0.307	0.164	0.347	0.241	0.087	0.154
41.06392	-101.10609	119.1	215.7	951.10	8.67	2594	0.168	0.068	0.353	0.255	0.091	0.164
41.06411	-101.10699	43.5	238.8	951.25	11.34	2594	0.168	0.068	0.368	0.302	0.114	0.188
41.06579	-101.10723	28.4	426.2	954.50	4.01	2601	0.193	0.100	0.350	0.251	0.081	0.170

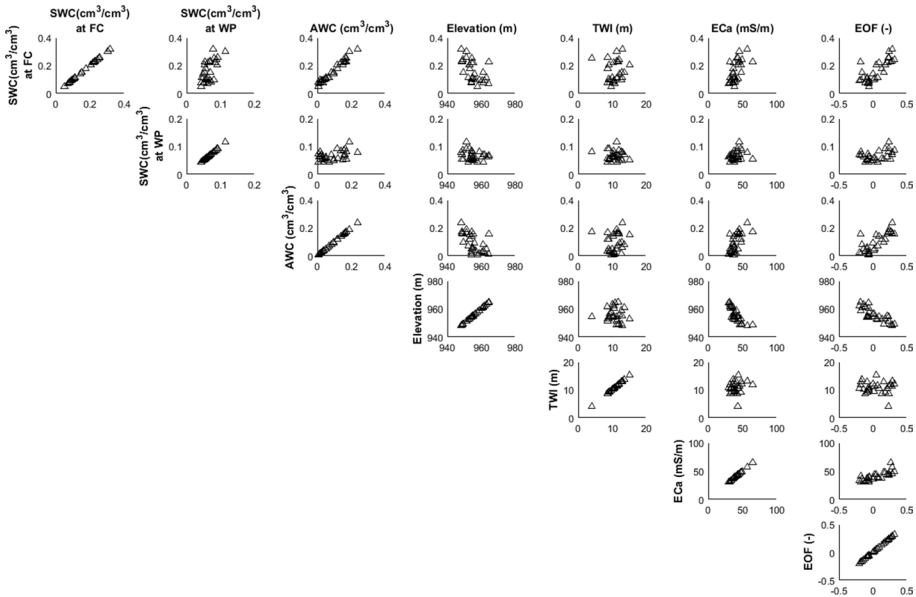


Fig. 8 Laboratory measured SWC at field capacity (FC) and wilting point (WP) compared to AWC, elevation, TWI, measured ECa, and the first EOF surface from the CRNP rover SWC surveys

the soil water retention curves generated using the Hyprop and WP4C instruments. Table 3 summarizes the linear correlation coefficient (r^2) and root mean square error (RMSE) for the graphs illustrated in Fig. 8. The first EOF coefficients have the largest linear correlation coefficient (r^2) with calculated AWC, laboratory measured SWC at field capacity and laboratory measured SWC at wilting point (Table 3). Compared to ECa, the CRNP and EOF analysis increased the linear correlation r^2 by 0.218 and reduced the RMSE by $0.012 \text{ cm}^3 \text{ cm}^{-3}$ for measured SWC at field capacity. Table 3 exemplifies the weak relationship between laboratory measured SWC at field capacity and elevation, laboratory measured SWC at wilting point and elevation, calculated AWC and elevation, laboratory measured SWC at field capacity and TWI, laboratory measured SWC at wilting point and TWI, and calculated AWC and TWI. Therefore, the hypothesis that the first EOF provides superior spatial information correlating to the accurate prediction of three key soil hydraulic parameters (i.e. field capacity, wilting point, available water content) is justified for this field.

In addition to providing more accurate soil hydraulic property spatial datasets, EOFs can be used to generate new data products for use with variable-rate irrigation (VRI), variable-speed irrigation (VSI), and other commercial field equipment. As an illustration here, new field capacity, wilting point and AWC products were generated for this field using the relationships between the first EOF surface, elevation, and the laboratory measured hydraulic parameters (Fig. 9, Table 3). The authors note that additional single or multivariate linear/nonlinear functions could be explored to better characterize the observed trends in the data.

In the interest of exploring the feasibility of implementing CRNP and EOF analysis for the delineation of IMZs, a statistical bootstrapping analysis was performed (Table 4) to predict the number of soil samples needed to accurately estimate field capacity, wilting point and AWC following a similar analysis by Gibson and Franz (2018). Each of the hydrogeophysical datasets (elevation, ECa survey, CRNP neutron count EOF, CRNP SWC

Table 3 Linear regression r^2 and RMSE for measured SWC at field capacity, measured SWC at wilting point and calculated AWC versus elevation, TWI, the ECa map and the first EOF surface

	Elevation (m)	TWI (m)	ECa (mSm^{-1})	EOF (-)	ECa (mSm^{-1})+Eleva- tion (m)	EOF (-)+Elevation (m)
SWC at field capacity (cm^3/cm^3)	$r^2 = 0.297$, RMSE = 0.064	$r^2 = 0.005$, RMSE = 0.076	$r^2 = 0.385$, RMSE = 0.060	$r^2 = 0.603$, RMSE = 0.048	$r^2 = 0.393$, RMSE = 0.061	$r^2 = 0.630$, RMSE = 0.047
SWC at wilting point (cm^3/cm^3)	$r^2 = 0.047$, RMSE = 0.016	$r^2 = 0.011$, RMSE = 0.017	$r^2 = 0.070$, RMSE = 0.016	$r^2 = 0.166$, RMSE = 0.015	$r^2 = 0.070$, RMSE = 0.017	$r^2 = 0.210$, RMSE = 0.015
AWC (cm^3/cm^3)	$r^2 = 0.321$, RMSE = 0.055	$r^2 = 0.012$, RMSE = 0.067	$r^2 = 0.411$, RMSE = 0.051	$r^2 = 0.613$, RMSE = 0.042	$r^2 = 0.422$, RMSE = 0.052	$r^2 = 0.632$, RMSE = 0.041

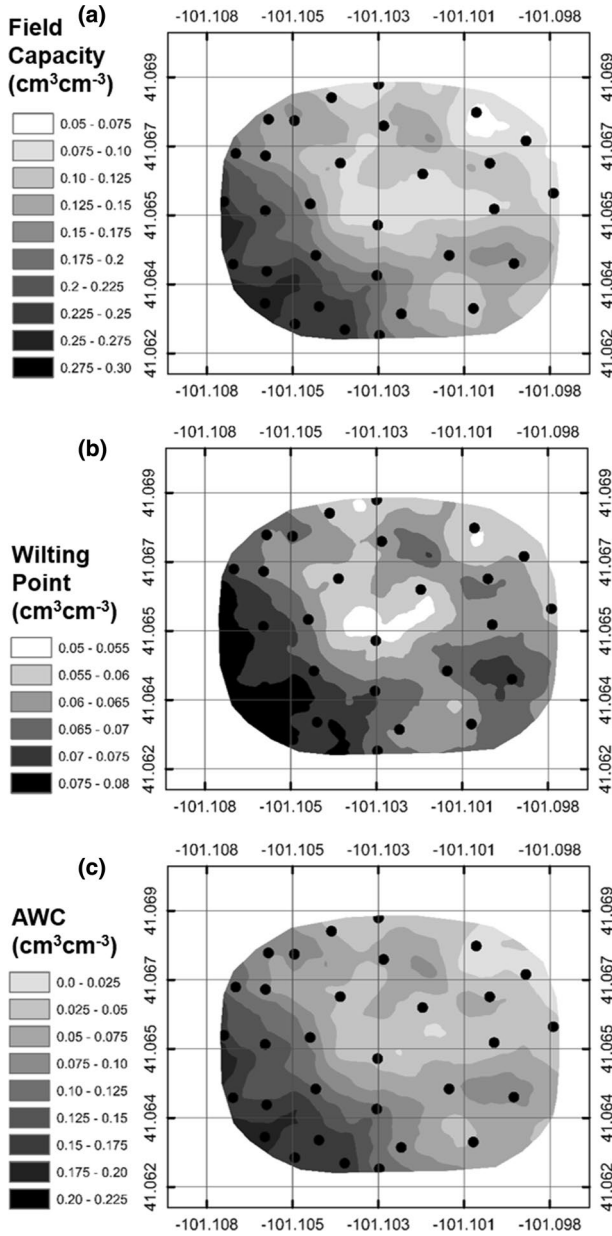


Fig. 9 Resulting spatial estimates of **a** SWC at field capacity ($FC = -4.314 + 0.473(\text{EOF}) + 0.005(\text{Elevation})$), **b** SWC at wilting point ($WP = -1.182 + 0.073(\text{EOF}) + 0.001(\text{Elevation})$) and **c** AWC ($AWC = -3.132 + 0.399(\text{EOF}) + 0.003(\text{Elevation})$) using derived relationships between the first EOF surface, elevation and the laboratory measured soil hydraulic parameters. The soil sampling locations are indicated by black circles and the corresponding r^2 and RMSE values for each of the spatial products are located in Table 3. See Table 4 for bootstrap analysis quantifying statistical fit and number of training and validation samples

Table 4 Results from the bootstrapping analysis

Hydrogeophysical dataset	Training set size	SWC at field capacity (cm ³ /cm ³)		SWC at wilting point (cm ³ /cm ³)		AWC (cm ³ /cm ³)	
		RMSE	SD	RMSE	SD	RMSE	SD
SWC EOF	3	0.0653	0.0235	0.0203	0.0070	0.0551	0.0192
SWC EOF	4	0.0638	1.2390	0.0202	0.3940	0.0537	1.0155
SWC EOF	5	0.0542	0.0691	0.0173	0.0244	0.0466	0.0697
SWC EOF	6	0.0529	0.0359	0.0169	0.0085	0.0454	0.0341
SWC EOF	7	0.0521	0.0256	0.0167	0.0054	0.0447	0.0220
SWC EOF	8	0.0516	0.0191	0.0166	0.0053	0.0443	0.0175
SWC EOF	9	0.0512	0.0105	0.0164	0.0035	0.0440	0.0135
SWC EOF	10	0.0509	0.0098	0.0164	0.0034	0.0437	0.0068
SWC EOF	20	0.0488	0.0103	0.0158	0.0026	0.0417	0.0095
SWC EOF	30	0.0460	0.0221	0.0149	0.0053	0.0386	0.0204
Neutron EOF	3	0.0671	0.0224	0.0202	0.0067	0.0564	0.0186
Neutron EOF	4	0.0657	1.4190	0.0201	0.3348	0.0551	1.1464
Neutron EOF	5	0.0545	0.0682	0.0173	0.0227	0.0469	0.0701
Neutron EOF	6	0.0532	0.0300	0.0169	0.0077	0.0457	0.0265
Neutron EOF	7	0.0525	0.0163	0.0167	0.0057	0.0451	0.0207
Neutron EOF	8	0.0521	0.0173	0.0166	0.0043	0.0447	0.0126
Neutron EOF	9	0.0517	0.0128	0.0165	0.0033	0.0444	0.0100
Neutron EOF	10	0.0513	0.0097	0.0164	0.0028	0.0441	0.0076
Neutron EOF	20	0.0491	0.0103	0.0158	0.0025	0.0421	0.0096
Neutron EOF	30	0.0458	0.0212	0.0151	0.0055	0.0394	0.0210
ECa	3	0.0788	0.0224	0.0222	0.0064	0.0695	0.0194
ECa	4	0.0779	0.7268	0.0222	0.4195	0.0686	0.8176
ECa	5	0.0689	0.0982	0.0188	0.0274	0.0590	0.1063
ECa	6	0.0672	0.0467	0.0184	0.0087	0.0572	0.0450
ECa	7	0.0662	0.0281	0.0182	0.0069	0.0563	0.0225
ECa	8	0.0656	0.0181	0.0180	0.0056	0.0558	0.0167
ECa	9	0.0652	0.0145	0.0179	0.0044	0.0554	0.0133
ECa	10	0.0648	0.0135	0.0178	0.0041	0.0551	0.0111
ECa	20	0.0627	0.0093	0.0172	0.0034	0.0535	0.0076
ECa	30	0.0605	0.0222	0.0166	0.0073	0.0518	0.0176
Elevation	3	0.0841	0.0225	0.0214	0.0071	0.0742	0.0197
Elevation	4	0.0833	1.2948	0.0214	0.3674	0.0735	1.2446
Elevation	5	0.0729	0.1050	0.0182	0.0222	0.0627	0.1071
Elevation	6	0.0711	0.1062	0.0178	0.0128	0.0611	0.0404
Elevation	7	0.0700	0.0230	0.0175	0.0062	0.0602	0.0220
Elevation	8	0.0695	0.0177	0.0174	0.0050	0.0597	0.0141
Elevation	9	0.0690	0.0131	0.0173	0.0043	0.0594	0.0116
Elevation	10	0.0686	0.0130	0.0172	0.0035	0.0591	0.0104
Elevation	20	0.0663	0.0102	0.0166	0.0027	0.0570	0.0094
Elevation	30	0.0626	0.0236	0.0156	0.0058	0.0537	0.0218

The hydrogeophysical datasets (EOF derived from CRNP SWC estimates, EOF derived from the CRNP corrected neutron counts, ECa values and Elevation) were divided into different training sets and the mean RMSE and standard deviations (SD) of the RMSE of the predicted soil hydraulic properties and the laboratory measured soil hydraulic properties are reported for 1000 random simulations. Note the total sample size was 31

EOF) was randomly divided into training and testing sets, with training set sizes ranging from 3 to 30, for 1000 iterations. The results from Table 4 suggest with fewer soil samples the neutron and SWC EOF surfaces are a more accurate predictor of soil hydraulic properties. When linearly correlating the CRNP SWC EOF to estimates of SWC at field capacity and AWC, RMSE is reduced approximately 20–25% compared to evaluations with ECa and elevation datasets. Wilting point estimates saw reductions in RMSE of 5–9% when comparing the CRNP SWC EOF to ECa and elevation datasets. Here, 6–8 sample locations for laboratory analysis were sufficient to describe the spatial distribution of soil hydraulic properties for this field. After eight soil samples, relatively small reductions in RMSE and standard deviation occurred for this particular field. Similar soil sampling sizes and results were found by Gibson and Franz (2018).

Recommendations for future soil hydraulic property sampling

Given the results of this work the authors propose a sampling strategy for better quantifying soil hydraulic properties that can be implemented in practice.

- (1) Complete a minimum of five CRNP rover surveys for the area of interest, with survey datasets selected to capture a range of SWC, to accurately estimate spatial SWC using the first one or two sets of EOF coefficients. As previously stated, the presented work used a bootstrapping analysis to indicate five CRNP surveys at different SWC conditions were sufficient to estimate the first EOF coefficients to within 5% of the values using data from all ten surveys. The five CRNP surveys and EOF correlations from this work are further supported by Gibson and Franz (2018). EOF coefficients could be calculated based on the neutron intensity measurements (Table 4), saving processing time and eliminating the need for terrestrial hydrogen pool datasets. However, the authors suggest using the CRNP SWC product as it has a greater physical meaning to soil hydraulic properties. Based on additional data (Gibson and Franz 2018) from fields across the Midwest, the authors found similar relationships and recommendations for the required minimal number of CRNP surveys. An example of real-world implementation might involve a service provider investing in CRNP technology and cooperating with multiple producers to perform the CRNP rover surveys. Additionally, the CRNP surveys could be completed simultaneously with other field operations (i.e. ATV, tractor, sprayer) and over several growing seasons.
- (2) Using the EOF coefficients from the CRNP SWC maps, 6–8 soil sample locations (Table 4) should be selected across a range of EOF values. The collection and analysis of soil cores to determine their soil retention curves and hydraulic parameters can be time consuming, laborious and expensive. Therefore, using the EOF surface to minimize the number of and placement of extracted soil cores is critical. The bootstrap analyses indicated a diminishing return of information beyond 6–8 samples for this 53 ha field. Similar sample sizes were reported in Gibson and Franz (2018).
- (3) Next, measure the soil hydraulic properties of interest (e.g. field capacity, wilting point, AWC) for the collected soil samples. Soil samples can be sent to a soil laboratory or analyzed in one's lab using the Hyprop/WP4C combination for this work.
- (4) New data products can be generated using the relationship between EOF and the observed hydraulic parameters from the soil cores. These new data products can be produced at a variety of scales and different file types to operate within existing agricultural software and machinery.

- (5) In addition, the EOF surface can be used to delineate management zones. Here the authors suggest using a 1st order polynomial relationship describing the relationship between the first SWC EOF surface, elevation, and the laboratory measured SWC at field capacity ($r^2=0.63$, $RMSE=0.05 \text{ cm}^3 \text{ cm}^{-3}$) and wilting point ($r^2=0.21$, $RMSE=0.02 \text{ cm}^3 \text{ cm}^{-3}$) to delineate IMZs (Table 3). This should be done in conjunction with the USDA SSURGO data to better refine key boundaries. IMZs can be based on the EOF surface, the field capacity surface or the AWC surface.

This research is of increasing importance for agricultural regions with ever-increasing water restrictions where small changes in water allocation rates and times may greatly impact crop yields. For example, at the current depletion rate, 35% of the Southern High Plains Aquifer is expected to be unable to support irrigation in the next 30 years (Scanlon et al. 2012). Consequently, there will be an increased effort to accurately map soil hydraulic properties and delineate high spatial and temporal irrigation prescription maps. Referring to Fig. 1, the feasibility of the CRNP and EOF analyses for management practice may soon be economically viable for many regions where maximizing water use for obtaining higher yields is paramount. The authors have shown here that the strong correlation with observed soil hydraulic parameters to the first EOF surface provides additional spatial variability information compared to EC mapping alone. If a land manager only used an EC map for estimating soil hydraulic properties, areas of a field may be biased depending on conditions at the time of sampling. In order to minimize error and improve IMZs, CRNP and EOF analysis should be used to increase the correlation between soil hydraulic properties and irrigation application rates (Fig. 8, Table 3), which will subsequently improve irrigation prescription maps. CRNP and EOF analysis also provides irrigators with datasets they can use to generate dynamic prescription irrigation maps. Future research could investigate how increases in r^2 and reductions in RMSE using the CRNP and EOF analysis could translate into increased water use efficiency with precision agricultural technologies. Additionally, studies could investigate whether high spatial resolution datasets of soil hydraulic properties increase water use efficiency while maintaining or increasing crop yields.

Summary and conclusions

Irrigation constitutes the largest component in global water use, yet within agricultural systems there is low water use efficiency. Therefore, improvements can be made in how irrigation application rates and times are managed. Traditional methods include the use of available soil property datasets, EC mapping, or commercially available instruments to delineate irrigation and land management zones. This research explored the utility of a hydrogeophysical sensor, called the CRNP, which measures near-surface soil water content (SWC) (top~30 cm). In addition, when combining the CRNP SWC maps with the multivariate EOF analysis the authors found a better covariate for laboratory measured soil hydraulic properties for a field in west-central Nebraska, USA. The measured soil hydraulic properties were also compared to other readily available landscape and geophysical datasets including elevation, TWI and ECa maps. Based on this work the authors present a future sampling strategy to better understand spatially varying hydraulic properties within a field, as well as the delineation of IMZs. The new data products could be used within current irrigation management practice to improve water use efficiency by providing soil spatial datasets for the management of irrigation rates and times in relation to depletion below

field capacity and above wilting point. Having an accurate quantification of field capacity and wilting point is especially important when volumetric SWC sensors are used for irrigation management. The authors do note that the strategy presented here constitutes a significant increase in effort as compared to more traditional and widely used techniques. However, as irrigation allocations become more stringent, there will likely be an increased rate of adoption of precision techniques that require more accurate mapping of soil hydraulic properties. The technology and framework presented here provides one potential strategy to better utilize precision agricultural technologies to increase water use efficiency while maintaining crop yields in varying topo-edaphic landscapes.

Acknowledgements This research was supported by the University of Nebraska Extension. The authors would also like to thank Paulman Farms for access to the field site and historical datasets and Matthew Russell for assistance collecting soil samples. TEF, DMH, and JL would also like to acknowledge the financial support of the United States Department of Agriculture National Institute of Food and Agriculture, Hatch Project #1009760. Trade names or commercial products are given solely for the purpose of providing information on the exact equipment used in this study and do not imply recommendation or endorsement by the University of Nebraska.

Compliance with ethical standards

Conflict of interest The authors declare that they have no conflict of interest.

References

- Binley, A., Hubbard, S. S., Hulsman, J. A., Revil, A., Robinson, D. A., Singha, K., et al. (2015). The emergence of hydrogeophysics for improved understanding of subsurface processes over multiple scales. *Water Resources Research*, *51*(6), 3837–3866. <https://doi.org/10.1002/2015wr017016>.
- Bobryk, C. W., Myers, D. B., Kitchen, N. R., Shanahan, J. F., Sudduth, K. A., Drummond, S. T., et al. (2016). Validating a digital soil map with corn yield data for precision agriculture decision support. *Agronomy Journal*, *108*(3), 957–965. <https://doi.org/10.2134/agnonj2015.0381>.
- Bogena, H. R., Huisman, J. A., Baatz, R., Franssen, H. J. H., & Vereecken, H. (2013). Accuracy of the cosmic-ray soil water content probe in humid forest ecosystems: The worst case scenario. *Water Resources Research*, *49*(9), 5778–5791. <https://doi.org/10.1002/wrcr.20463>.
- Brevik, E. C., Fenton, T. E., & Lazari, A. (2006). Soil electrical conductivity as a function of soil water content and implications for soil mapping. *Precision Agriculture*, *7*(6), 393–404. <https://doi.org/10.1007/s11119-006-9021-x>.
- Campbell, R. B., Bower, C. A., & Richards, L. A. (1948). Change of electrical conductivity with temperature and the relation of osmotic pressure to electrical conductivity and ion concentration for soil extracts. *Soil Science Society of America Proceedings*, *13*, 66–69.
- Chan, S., Njoku, E. G. & Colliander A. (2014). *Soil Moisture Active Passive (SMAP), Algorithm Theoretical Basis Document, Level 1C Radiometer Data Product, Revision A*. Jet Propulsion Laboratory, California Institute of Technology, Pasadena, CA. Retrieved 15 February, 2017 from <http://smap.jpl.nasa.gov/>.
- Coopersmith, E. J., Cosh, M. H., & Daughtry, C. S. T. (2014). Field-scale moisture estimates using COSMOS sensors: A validation study with temporary network and Leaf-Area-Indices. *Journal of Hydrology*, *519*, 637–643. <https://doi.org/10.1016/j.hydrol.2014.07.060>.
- Decagon Devices, Inc. (2015). WP4C dewpoint potentiometer operator's manual. Pullman, WA.
- Evans, R.G., Han, S., Kroeger, M.W., & Schneider, S. M. (1996). Precision center pivot irrigation for efficient use of water and nitrogen. In: P. C. Robert, R. H. Rust, & W.E. Larson (Eds.), *Precision agriculture* (pp. 75–84). ASA, CSSA, SSSA, Madison, WI. <https://doi.org/10.2134/1996.precisionagproc3.c8>
- Franz, T. E., King, E. G., Caylor, K. K., & Robinson, D. A. (2011). Coupling vegetation organization patterns to soil resource heterogeneity in a central Kenyan dryland using geophysical imagery. *Water Resources Research*. <https://doi.org/10.1029/2010wr010127>.

- Franz, T. E., Wahbi, A., Vreugdenhil, M., Weltin, G., Heng, L., Oismueller, M., et al. (2016). Using cosmic-ray neutron probes to monitor landscape scale soil water content in mixed land use agricultural systems. *Applied and Environmental Soil Science*. <https://doi.org/10.1155/2016/4323742>.
- Franz, T. E., Wang, T., Avery, W., Finkenbiner, C., & Brocca, L. (2015). Combined analysis of soil moisture measurements from roving and fixed cosmic-ray neutron probes for multiscale real-time monitoring. *Geophysical Research Letters*, 42(9), 3389–3396. <https://doi.org/10.1002/2015gl063963>.
- Franz, T. E., Zreda, M., Rosolem, R., & Ferre, P. A. (2012). Field validation of cosmic-ray soil moisture sensor using a distributed sensor network. *Vadose Zone Journal*. <https://doi.org/10.2136/vzj2012.0046>.
- Gibson, J., & Franz, T. E. (2018). Spatial prediction of near surface soil water retention functions using hydrogeophysics and empirical orthogonal functions. *Journal of Hydrology*. <https://doi.org/10.1016/j.jhydrol.2018.03.046>.
- Glasstone, S., & Edlund, M. C. (1952). *Elements of nuclear reactor theory*. New York: Van Nostrand.
- Haghverdi, A., Leib, B. G., Washington-Allen, R. A., Ayers, P. D., & Buschermohle, M. J. (2015a). High-resolution prediction of soil available water content within the crop root zone. *Journal of Hydrology*, 520, 167–179. <https://doi.org/10.1016/j.jhydrol.2015.09.061>.
- Haghverdi, A., Leib, B. G., Washington-Allen, R. A., Ayers, P. D., & Buschermohle, M. J. (2015b). Perspectives on delineating management zones for variable rate irrigation. *Computers and Electronics in Agriculture*, 117, 154–167. <https://doi.org/10.1016/j.compag.2015.06.019>.
- Hawdon, A., McJannet, D., & Wallace, J. (2014). Calibration and correction procedures for cosmic-ray neutron soil moisture probes located across Australia. *Water Resources Research*, 50(6), 5029–5043. <https://doi.org/10.1002/2013wr015138>.
- Hedley, C. (2015). The role of precision agriculture for improved nutrient management on farms. *Journal of the Science of Food and Agriculture*, 95(1), 12–19. <https://doi.org/10.1002/jsfa.6734>.
- Hedley, C. B., Roudier, P., Yule, I. J., Ekanayake, J., & Bradbury, S. (2013). Soil water status and water table depth modelling using electromagnetic surveys for precision irrigation scheduling. *Geoderma*, 199, 22–29. <https://doi.org/10.1016/j.geoderma.2012.07.018>.
- Hezarjaribi, A., & Sourell, H. (2007). Feasibility study of monitoring the total available water content using non-invasive electromagnetic induction-based and electrode-based soil electrical conductivity measurements. *Irrigation and Drainage*, 56(1), 53–65. <https://doi.org/10.1002/ird.289>.
- Howell, T. A., Evett, S. R., O'Shaughnessy, S. A., Colaizzi, P. D., & Gowda, P. H. (2012). Advanced irrigation engineering: Precision and precise. *Journal of Agricultural Science and Technology*, A(2), 1–9.
- Inc, Dualem. (2013). *DUALEM-21S user's manual*. Milton: Dualem Inc.
- Iwema, J., Rosolem, R., Rahman, M., Blyth, E., & Wagener, T. (2017). Land surface model performance using cosmic-ray and point-scale soil moisture measurements for calibration. *Hydrology and Earth System Sciences*, 21, 2843–2861. <https://doi.org/10.5194/hess-21-2843-2017>.
- Köhli, M., Schrön, M., Zreda, M., Schmidt, U., Dietrich, P., & Zacharias, S. (2015). Footprint characteristics revised for field-scale soil moisture monitoring with cosmic-ray neutrons. *Water Resources Research*, 51(7), 5772–5790. <https://doi.org/10.1002/2015wr017169>.
- Korres, W., Koyama, C. N., Fiener, P., & Schneider, K. (2010). Analysis of surface soil moisture patterns in agricultural landscapes using empirical orthogonal functions. *Hydrology and Earth System Sciences*, 14(5), 751–764. <https://doi.org/10.5194/hess-14-751-2010>.
- Martini, E., Werban, U., Zacharias, S., Pohle, M., Dietrich, P., & Wollschläger, U. (2016). Repeated electromagnetic induction measurements for mapping soil moisture at the field scale: Validation with data from a wireless soil moisture monitoring network. *Hydrology and Earth System Sciences*, 21, 495–513. <https://doi.org/10.5194/hess-21-495-2017>.
- McCarthy, A. C., Hancock, N. H., & Raine, S. R. (2014). Development and simulation of sensor-based irrigation control strategies for cotton using the VARIwise simulation framework. *Computers and Electronics in Agriculture*, 101, 148–162. <https://doi.org/10.1016/j.compag.2013.12.014>.
- McCutcheon, M. C., Farahani, H. J., Stednick, J. D., Buchleiter, G. W., & Green, T. R. (2006). Effect of soil water on apparent soil electrical conductivity and texture relationships in a dryland field. *Bio-systems Engineering*, 94(1), 19–32. <https://doi.org/10.1016/j.biosystemseng.2006.01.002>.
- McJannet, D., Franz, T., Hawdon, A., Boadle, D., Baker, B., Almeida, A., et al. (2014). Field testing of the universal calibration function for determination of soil moisture with cosmic-ray neutrons. *Water Resources Research*, 50(6), 5235–5248. <https://doi.org/10.1002/2014wr015513>.
- Molden, D. (2007). Water responses to urbanization. *Paddy and Water Environment*, 5(4), 207–209. <https://doi.org/10.1007/s11033-007-0084-8>.
- Pan, L., Adamchuk, V. I., Martin, D. L., Schroeder, M. A., & Ferguson, R. B. (2013). Analysis of soil water availability by integrating spatial and temporal sensor-based data. *Precision Agriculture*, 14(4), 414–433. <https://doi.org/10.1007/s11119-013-9305-x>.

- Perry, M. A., & Niemann, J. D. (2006). Analysis and estimation of soil moisture at the catchment scale using EOFs. *Journal of Hydrology*, 334(3–4), 388–404. <https://doi.org/10.1016/j.jhydrol.2006.10.014>.
- Peters, A., & Durner, W. (2008). Simplified evaporation method for determining soil hydraulic properties. *Journal of Hydrology*, 356(1–2), 147–162. <https://doi.org/10.1016/j.jhydrol.2008.04.016>.
- Ranney, K. J., Niemann, J. D., Lehman, B. M., Green, T. R., & Jones, A. S. (2015). A method to down-scale soil moisture to fine resolutions using topographic, vegetation, and soil data. *Advances in Water Resources*, 76, 81–96. <https://doi.org/10.1016/j.advwatres.2014.12.003>.
- Rivera Villarreyes, C. A., Baroni, G., & Oswald, S. E. (2011). Integral quantification of seasonal soil moisture changes in farmland by cosmic-ray neutrons. *Hydrology and Earth System Sciences*, 15, 3843–3859. <https://doi.org/10.5194/hess-15-3843-2011>.
- Rodríguez-Pérez, J. R., Plant, R. E., Lambert, J.-J., & Smart, D. R. (2011). Using apparent soil electrical conductivity (ECa) to characterize vineyard soils of high clay content. *Precision Agriculture*, 12(6), 775–794. <https://doi.org/10.1007/s11119-011-9220-y>.
- Scanlon, B. R., Faunt, C. C., Longuevergne, L., Reedy, R. C., Alley, W. M., McGuire, V. L., et al. (2012). Groundwater depletion and sustainability of irrigation in the US High Plains and Central Valley. *Proceedings of the National Academy of Sciences of the United States of America*, 109(24), 9320–9325. <https://doi.org/10.1073/pnas.1200311109>.
- Schindler, U., Durner, W., von Unold, G., Mueller, L., & Wieland, R. (2010). The evaporation method: Extending the measurement range of soil hydraulic properties using the air-entry pressure of the ceramic cup. *Journal of Plant Nutrition and Soil Science*, 173(4), 565–572. <https://doi.org/10.1002/jpln.200900201>.
- Schrön, M., Köhli, M., Scheffele, L., Iwema, J., Bogena, H. R., Lv, L., et al. (2017). Improving calibration and validation of cosmic-ray neutron sensors in the light of spatial sensitivity. *Hydrology and Earth System Sciences*, 21, 5009–5030. <https://doi.org/10.5194/hess-21-5009-2017>.
- Schultz, B., Thatte, C. D., & Labhsetwar, V. K. (2005). Irrigation and drainage: Main contributors to global food production. *Irrigation and Drainage*, 54, 263–278.
- Shangguan, W., Dai, Y., Duan, Q., Liu, B., & Yuan, H. (2014). A global soil data set for earth system modeling. *Journal of Advances in Modeling Earth Systems*, 6, 249–263. <https://doi.org/10.1002/2013MS000293>.
- Soil Survey Staff (2016) Natural Resources Conservation Service, United States Department of Agriculture. Soil Survey Geographic (SSURGO) Database. Retrieved 1 February, 2016 from <https://sdmdataaccess.sc.egov.usda.gov>.
- Sorensen, R., Zinko, U., & Selbert, J. (2006). On the calculation of the topographic wetness index: Evaluation of different methods based on field observations. *Hydrology and Earth System Sciences*, 10, 101–112.
- UNDP. (2007). *Human Development Report 2006-Beyond scarcity: Power, poverty and the global water crisis*. New York: United Nations Development Programme.
- USDA NASS. (2012). Census of agriculture. United States Department of Agriculture. Retrieved 2 April, 2018 https://www.agcensus.usda.gov/Publications/2012/Full_Report/Volume_1,_Chapter_1_US/usv1.pdf.
- Werbylo, K. L., & Niemann, J. D. (2014). Evaluation of sampling techniques to characterize topographically-dependent variability for soil moisture downscaling. *Journal of Hydrology*, 516, 304–316. <https://doi.org/10.1016/j.jhydrol.2014.01.030>.
- Zreda, M., Shuttleworth, W. J., Zeng, X., Zweck, C., Desilets, D., Franz, T., et al. (2012). COSMOS: The Cosmic-ray Soil Moisture Observing System. *Hydrology and Earth System Sciences*, 16(11), 4079–4099. <https://doi.org/10.5194/hess-16-4079-2012>.